

Research Article

Identifying Nonstationary Clock Noises in Navigation Systems

Lorenzo Galleani¹ and Patrizia Tavella²

¹ Politecnico di Torino, Corso Duca degli Abruzzi 24, 10129 Torino, Italy

² INRIM, Strada della Cacce 91, 10135 Torino, Italy

Correspondence should be addressed to Lorenzo Galleani, galleani@polito.it

Received 9 August 2007; Accepted 27 December 2007

Recommended by Demetrios Matsakis

The stability of the atomic clocks on board the satellites of a navigation system should remain constant with time. In reality, there are numerous physical phenomena that make the behavior of the clocks a function of time, and for this reason we have recently introduced the dynamic Allan variance (DAVAR), a measure of the time-varying stability of an atomic clock. In this paper, we discuss the dynamic Allan variance for phase and frequency jumps, two common nonstationarities of atomic clocks. The analysis of both numerical simulations and experimental data proves that the dynamic Allan variance is an effective way of characterizing nonstationary behaviors of atomic clocks.

Copyright © 2008 L. Galleani and P. Tavella. This is an open access article distributed under the Creative Commons Attribution License, which permits unrestricted use, distribution, and reproduction in any medium, provided the original work is properly cited.

1. INTRODUCTION

Navigation is certainly one of the most effective applications of atomic clocks. The exceptional stability of an atomic clock allows to reduce the localization error below one meter, as required, for example, by the Galileo system specifications. To guarantee and *maintain in time* a very high stability of the atomic clocks is therefore a fundamental requirement of a navigation system. Unfortunately, the stability of an atomic clock changes with time as a consequence of several different phenomena: sudden and cyclic variations of temperature, aging of physical devices, sudden breakdowns are among the main causes of nonstationarities.

It is hence necessary to introduce a tool that allows to represent the stability of an atomic clock as a function of time. We have recently proposed the *dynamic Allan variance*, or DAVAR, a quantity that measures the time-varying stability of a clock by sliding the classical Allan variance on the data [1–4]. By using the dynamic Allan variance we are classifying the typical nonstationarities of atomic clocks that operate on board a satellite. The final goal is to identify the clock anomalies directly from the DAVAR, which can reveal variations in the stability that cannot be tracked with other methods [5]. In this way, proper warnings can be generated so that the integrity of the clock and of the satellite signal can be monitored continuously in time.

In this paper, we consider two typical nonstationarities of atomic clocks and we discuss the corresponding dynamic Allan variance. We also analyze experimental data that show the anomalies described.

2. THE DYNAMIC ALLAN VARIANCE

Time series from atomic clocks are typically represented by the phase deviation (we use bold symbols for stochastic quantities) $\mathbf{x}(t)$, or by the normalized frequency deviation $\mathbf{y}(t)$ [6]:

$$\mathbf{y}(t) = \frac{d\mathbf{x}(t)}{dt}. \quad (1)$$

The stability of a clock is standardly defined through the Allan variance [7–10]

$$\sigma_{\mathbf{y}}^2(\tau) = \frac{1}{2} \langle (\bar{\mathbf{y}}_{t+\tau} - \bar{\mathbf{y}}_t)^2 \rangle, \quad (2)$$

where τ is the observation interval, the operator $\langle \cdot \rangle$ stands for time averaging, and $\bar{\mathbf{y}}_t$ is defined as

$$\bar{\mathbf{y}}_t(t) = \frac{1}{\tau} \int_{t-\tau}^t \mathbf{y}(t) dt = \frac{\mathbf{x}(t) - \mathbf{x}(t-\tau)}{\tau}. \quad (3)$$

In discrete-time we evaluate the Allan variance with the following estimator:

$$\hat{\sigma}_y^2[k] = \frac{1}{2k^2\tau_0^2} \frac{1}{N-2k} \sum_{n=0}^{N-2k-1} (\mathbf{x}[n+2k] - 2\mathbf{x}[n+k] + \mathbf{x}[n])^2, \quad (4)$$

where N is the total number of samples, $k = \tau/\tau_0$ is an integer number representing the discrete-time observation interval, and τ_0 is the minimum observation interval. To control the variance of the estimate that increases with k , one typically takes $k = 1, 2, \dots, k_{\max}$, where $k_{\max} = \lfloor N/3 \rfloor$, with N being the total number of samples (the symbol $\lfloor \cdot \rfloor$ stands for the integer part of the number).

The dynamic Allan variance is defined as

$$\begin{aligned} \sigma_y^2[n, k] &= \frac{1}{2k^2\tau_0^2} \frac{1}{N-2k} \\ &\times \sum_{m=n-N_w/2+k}^{n+N_w/2-k-1} E[(\mathbf{x}[m+k] - 2\mathbf{x}[m] + \mathbf{x}[m-k])^2], \end{aligned} \quad (5)$$

where $n = t/\tau_0$ is the discrete time and N_w is the length of the analysis window. In the definition we have used the expectation value $E[\cdot]$ because we wanted $\sigma_y^2[n, k]$ to be a deterministic quantity. In this way, we can study the properties of the DAVAR without taking into account the random fluctuations that are present every time that we consider one realization only of $\mathbf{x}[n]$.

The DAVAR is in practice obtained by sliding the estimator $\hat{\sigma}_y^2[k]$ of the Allan variance on the data. The DAVAR at time n is made by the Allan variance of the N_w samples centered about n . When analyzing experimental data, we apply the estimator

$$\begin{aligned} \hat{\sigma}_y^2[n, k] &= \frac{1}{2k^2\tau_0^2} \frac{1}{N-2k} \\ &\times \sum_{m=n-N_w/2+k}^{n+N_w/2-k-1} (\mathbf{x}[m+k] - 2\mathbf{x}[m] + \mathbf{x}[m-k])^2, \end{aligned} \quad (6)$$

which is identical to (5) except for the expectation value. We again take $k = 1, 2, \dots, k_{\max}$, with $k_{\max} = \lfloor N/3 \rfloor$ (other choices are possible). We also define the *dynamic Allan deviation* $\sigma_y[n, k]$, or *DADEV*, as the square root of the DAVAR (the DADEV estimator $\hat{\sigma}_y[n, k]$ is defined in an identical way).

There is a typical tradeoff in the computation of the dynamic Allan variance. If the window is long, the variance of the estimate is small, but the localization of events in time is poor. Conversely, a short window guarantees an excellent localization of events, but has a poor variance reduction. It is better to choose the window on a case-by-case basis, depending on the type of data considered.

3. ANALYSIS OF NONSTATIONARY CLOCK NOISES

We now consider two typical nonstationary behaviors of atomic clocks, namely, a phase and a frequency jump. Both

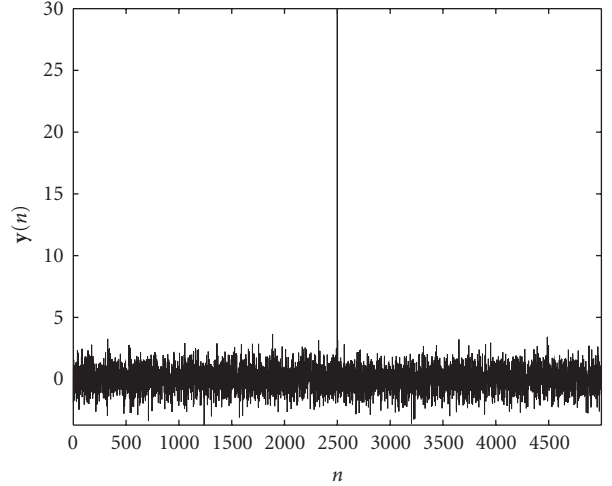


FIGURE 1: White frequency noise plus a delta function (7).

cases are studied using numerical simulations. The dynamic Allan variance is then applied to a set of experimental data that show the same types of nonstationarity.

3.1. Case 1: phase jump

It is very common for clocks on board satellites to experience jumps in the phase signal, which become spikes in the frequency deviation, since frequency is defined as the derivative of phase (see (1)). These frequency values are considered outliers, since they are numerically distant from the rest of the data. Outliers should be removed in the preprocessing of data, but since some of them could go unaltered through the removal algorithm, it is of practical importance to understand what they look like in the dynamic Allan variance domain.

Therefore, we consider a white frequency noise to which we add a delta function, and we numerically study the corresponding DAVAR. The signal model is

$$\mathbf{y}[n] = \mathbf{f}[n] + c\delta[n - n_0], \quad (7)$$

where $\mathbf{f}[n]$ is the usual white Gaussian noise, c is an arbitrary constant and n_0 is the discrete-time at which the delta function is located. The discrete-time delta function is defined as

$$\delta[n] = \begin{cases} 1, & n = 0, \\ 0, & n \neq 0. \end{cases} \quad (8)$$

In Figure 1, we show the resulting frequency $\mathbf{y}[n]$, where $n_0 = 2500$ and we have taken c to be 30 times the standard deviation of $\mathbf{y}[n]$. In Figure 2, we show the estimated Allan deviation $\hat{\sigma}_y[k]$ of $\mathbf{y}[n]$, where we see the typical slope of a white frequency noise, and we do not notice the delta function. In Figure 3, the estimated dynamic Allan deviation $\hat{\sigma}_y[n, k]$ is represented. We see that before and after the time instant n_0 , the DADEV surface is stationary, beside some obvious fluctuations due to the variance of the estimate. In the stationary regions, the slope indicates that locally $\mathbf{y}[n]$ is a

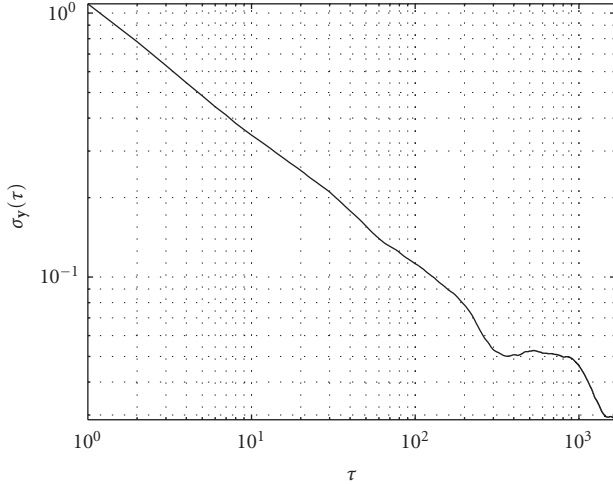


FIGURE 2: Allan deviation of the signal shown in Figure 1.

white frequency noise. Around $n = n_0$ we instead see a decrease in the stability (an increase in the dynamic Allan deviation surface), which takes place at all observation intervals. This change in the stability is due to the delta function in frequency, and is more intense as c increases. The reason we see a change in stability for all observation intervals is that at any k some of the triplets $\mathbf{x}[m+k]$, $\mathbf{x}[m]$, $\mathbf{x}[m-k]$ used in the DADEV computation include the delta function located at $n = n_0$. Since the value of the delta function is much bigger than the standard deviation of the stationary noise $\mathbf{f}[n]$, the corresponding triplets will be much bigger than those that are located outside the nonstationary region. This fact implies that the dynamic Allan deviation computed for the analysis times whose corresponding window include the time instant n_0 will be bigger than the DADEV that is computed on the stationary regions alone, which is precisely what we observe in Figure 3.

3.2. Case 2: frequency jump

Also frequency jumps can be detected in atomic clocks on board satellites. A simple model for a frequency jump is given by

$$\mathbf{y}[n] = \begin{cases} \mu_1 + \mathbf{f}[n], & n \leq n_0, \\ \mu_2 + \mathbf{f}[n], & n > n_0, \end{cases} \quad (9)$$

where $\mathbf{f}[n]$ is a white Gaussian noise with zero mean. The model of $\mathbf{y}[n]$ has been chosen so that the mean value is

$$\mu[n] = E[\mathbf{y}[n]] = \begin{cases} \mu_1, & n \leq n_0, \\ \mu_2, & n > n_0. \end{cases} \quad (10)$$

This means that there is a sudden variation in the mean of $\mathbf{y}[n]$, as shown in Figure 4. The estimated Allan deviation $\hat{\sigma}_y[k]$ is given in Figure 5. We see that the Allan deviation has the typical slopes of a white frequency noise, and that there is no evident trace of the nonstationarity going

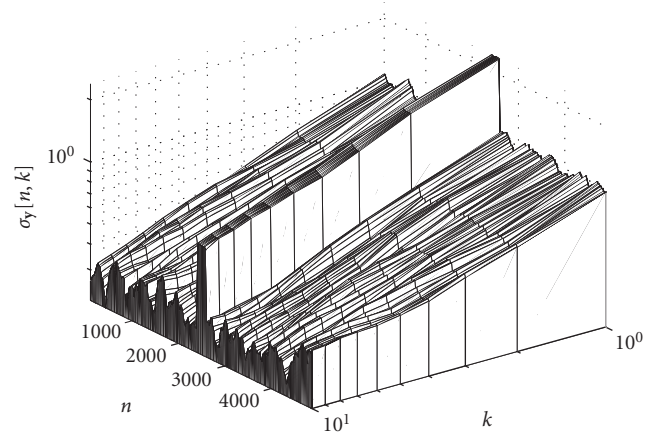


FIGURE 3: Dynamic Allan deviation of the signal shown in Figure 1.

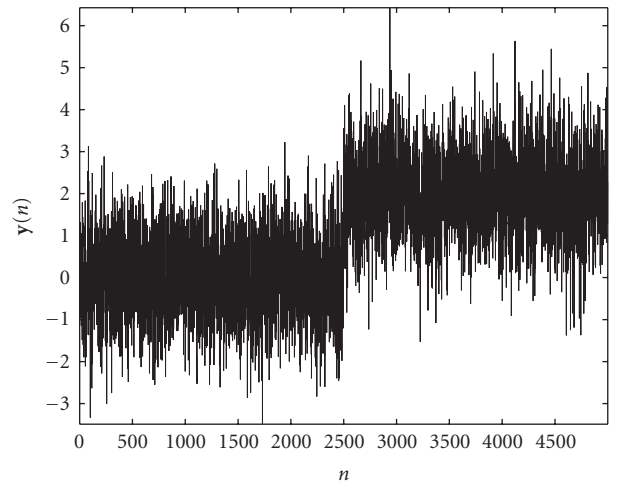


FIGURE 4: White frequency noise with a frequency jump (9).

on in the clock noise. The reason is that the jump in the mean value of the signal has been averaged out by the Allan variance. In Figure 6, we instead see the estimate $\hat{\sigma}_y[n, k]$ of the dynamic Allan deviation, computed with a window of $N_w = 200$ samples. We notice that for small values of the discrete observation interval k , the DADEV does not show the change in mean. The reason is that for small k values the frequency jump is present only in few of the triplets $\mathbf{x}[m+k]$, $\mathbf{x}[m]$, $\mathbf{x}[m-k]$ used in the DADEV estimation. Most of the triplets are located in the stationary regions before and after the discontinuity, and they are not influenced by the change in the mean. For increasing values of k we see that the stability steadily decreases. The reason is that for large k most of the triplets are made by values located before and after the nonstationarity, that will hence track the discontinuity in the mean.

3.3. Experimental data

We now analyze a set of experimental data coming from a Rubidium clock undergoing tests for space flight certification.

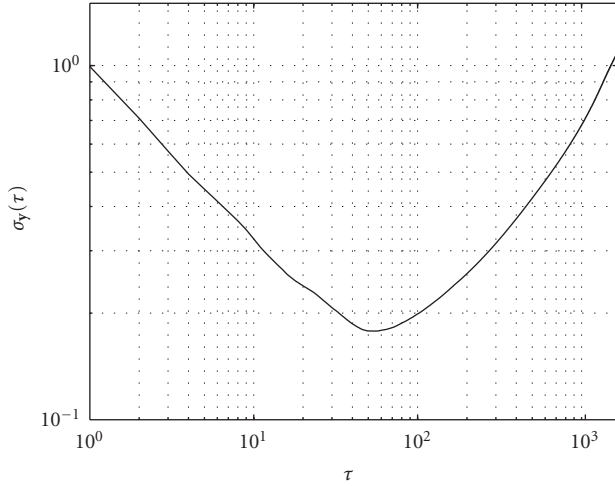


FIGURE 5: Allan deviation of the signal shown in Figure 4.

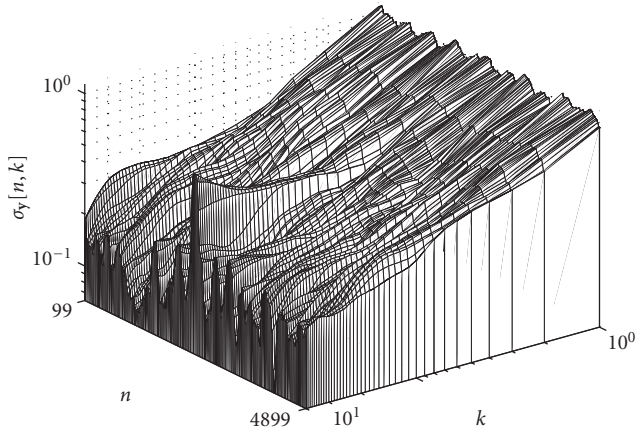


FIGURE 6: Dynamic Allan deviation of the signal shown in Figure 4.

In Figure 7, we show a section of the frequency data $\mathbf{y}(t)$. We notice a frequency jump located approximately at $t_1 = 1.6 \cdot 10^4$ seconds. After this sudden variation, $\mathbf{y}(t)$ gradually recovers a mean value close to the one that it had before the nonstationarity. There is also a spike in frequency located roughly at $t_2 = 3.9 \cdot 10^4$ seconds, which indicates that a jump in the phase $\mathbf{x}(t)$ has taken place at the same time instant.

In Figure 8, we see the Allan deviation $\hat{\sigma}_y[k]$ of $\mathbf{y}(t)$, which shows the typical slopes of a Rubidium clock and does not point out the presence of nonstationary behaviors. In Figure 9, we instead represent the dynamic Allan deviation. Around $t = t_1$ we notice that the DADEV surface increases for large τ values, which implies the presence of a step change in the mean of the frequency $\mathbf{y}(t)$, as discussed in Section 3.2. Also, around $t = t_2$ we see an increase in the DADEV for all τ values, which means that there is a spike in frequency or, equivalently, that there is a jump in the phase data $\mathbf{x}(t)$, as previously discussed in Section 3.1. Outside the regions around t_1 and t_2 the dynamic Allan deviation is mostly sta-

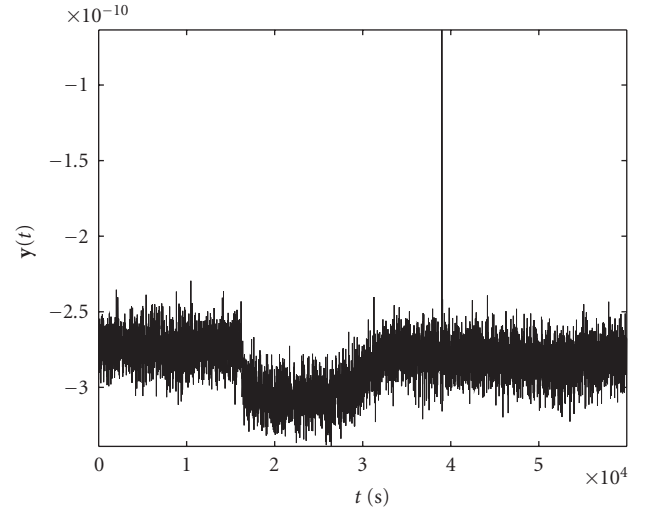


FIGURE 7: Frequency data of a Rubidium clock.

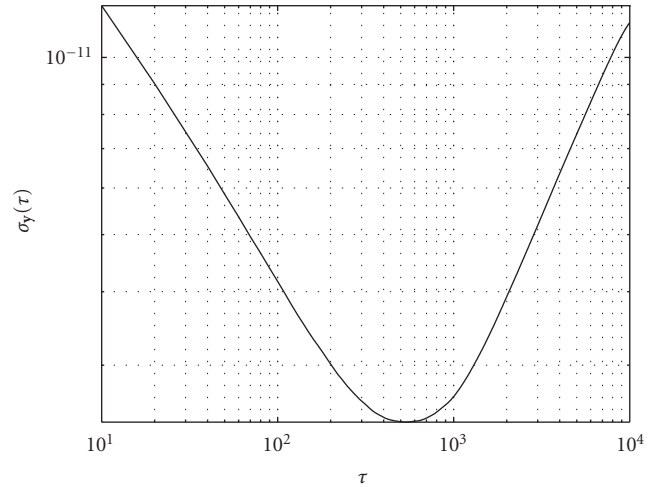


FIGURE 8: Allan deviation of the signal shown in Figure 7.

tionary and it is in accordance with the slope of a Rubidium clock.

It is therefore possible to characterize the stability of the Rubidium clock by directly observing the dynamic Allan variance surface.

4. CONCLUSION

Navigation requires atomic clocks on board the satellites to have a very high stability, and to maintain it with time. Since in reality there are several physical phenomena that produce variations in the clock behavior, it is fundamental to understand how its stability changes with time. For this reason we have proposed the dynamic Allan variance, or DAVAR, a quantity that is able to characterize the nonstationary behaviors of atomic clocks. In this paper, we have analyzed two typical nonstationarities that affect atomic clocks on board a satellite, namely, phase and frequency jumps. Numerical simulations demonstrate that the DAVAR

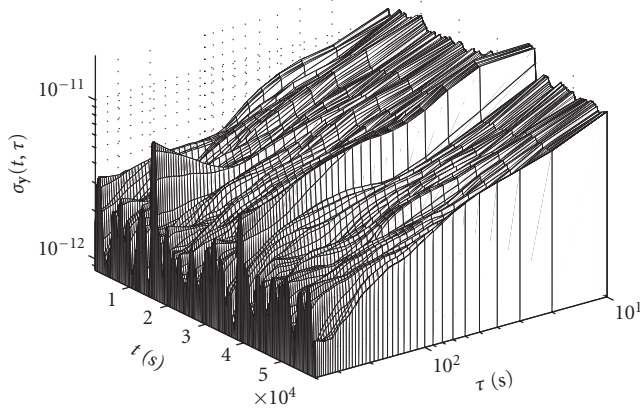


FIGURE 9: Dynamic Allan deviation of the signal shown in Figure 7.

correctly represents these anomalous behaviors. We have also validated our method with experimental data, proving that it is possible to understand the nonstationarities of a clock by directly inspecting the DAVAR surface. This means that it is possible to design anomaly detection methods directly in the dynamic Allan variance domain (a free Matlab implementation of the DAVAR can be found at www.ien.it/tf/ts/clock_behavior.shtml) [5].

REFERENCES

- [1] L. Galleani and P. Tavella, "Interpretation of the dynamic Allan variance of nonstationary clock data," in *Proceedings of IEEE International Frequency Control Symposium, Jointly with the 21st European Frequency and Time Forum (FREQ '07)*, pp. 992–997, Geneva, Switzerland, 2007 May–June.
- [2] L. Galleani and P. Tavella, "Tracking nonstationarities in clock noises using the dynamic Allan variance," in *Proceedings of the IEEE International Frequency Control Symposium and Exposition (FREQ '05)*, pp. 392–396, Vancouver, Canada, August 2005.
- [3] L. Galleani and P. Tavella, "The characterization of clock behavior with the dynamic Allan variance," in *Proceedings of IEEE International Frequency Control Symposium and PDA Exhibition Jointly with the 17th European Frequency and Time Forum (FREQ '03)*, pp. 239–244, Tampa, Fla, USA, May 2003.
- [4] I. Sesia, L. Galleani, and P. Tavella, "Implementation of the dynamic Allan variance for the Galileo system test bed V2," in *Proceedings of IEEE International Frequency Control Symposium, Jointly with the 21st European Frequency and Time Forum (FREQ '07)*, pp. 946–949, Geneva, Switzerland, 2007 May–June.
- [5] E. Nunzi, L. Galleani, P. Tavella, and P. Carbone, "Detection of anomalies in the behavior of atomic clocks," *IEEE Transactions on Instrumentation and Measurement*, vol. 56, no. 2, pp. 523–528, 2007.
- [6] P. Kartschoff, *Frequency and Time*, Academic Press, New York, NY, USA, 1978.
- [7] D. W. Allan, "Statistics of atomic frequency standards," *Proceedings of the IEEE*, vol. 54, no. 2, pp. 221–230, 1966.
- [8] "IEEE Standard Definitions of Physical Quantities for Fundamental Frequency and Time Metrology," IEEE Standards, 1139–199.
- [9] ITU Handbook, "Selection and use of precise frequency and time systems," International Telecommunication Union—Radiocommunication ITU-R, Geneva, Switzerland, 1997.
- [10] ITU-R Recommendation TF 538-3, "Measures for random instabilities in frequency and time (phase)," International Telecommunication Union—Radiocommunication ITU-R, volume 2000, TF Series, Geneva, Switzerland, 2001.



Hindawi

Submit your manuscripts at
<http://www.hindawi.com>

